Modelling and simulating the dynamics of in-stent restenosis in porcine coronary arteries

Tahir, H.

Publication date
2013

4

4. Effect of the origin of endothelium regeneration on In-stent Restenosis

In-stent restenosis (ISR) is the re-narrowing of the stented artery after percutaneous coronary intervention (PCI) [132,133]. In comparison to bare metal stents (BMS), drug eluting stents (DES) have dramatically reduced the rates of ISR [134]. In the era of DES, ISR is no longer regarded as a significant problem [133], however, a low rate of ISR occurrence still exists [134]. Despite of the reduction in ISR, DES have also been associated with a late stent thrombosis (LST), very late stent thrombosis (VLST) and re-infarction [17,18]. Additionally, delayed re-endothelialisation and vessel wall toxicity in the form of medial necrosis have been reported [17,19,20,21,22].

ISR, being an exaggerated response of the arterial tissue following balloon angioplasty and stent deployment, occurs in response to the mechanical changes (the injury) in the vascular wall. Balloon inflation is considered to damage or crush the endothelium whereas the sharpness of the stent struts is responsible for further damage to the internal elastic lamina and the medial tissue [29].

Tahir H, Bona-Casas C, Narracott A, Gunn J, Lawford PV, Iqbal J, Hoekstra AG Endothelial repair process and its relevance to longitudinal neointimal tissue patterns: Comparing histology with in-silico modelling. (Submitted to Cardiovascular Research, 2013)

The early phase of the injury involves denudation of endothelial cells (ECs) and the extent of endothelial damage can vary from a partial destruction to complete denudation. This damage activates a cascade of cellular processes that involves platelet activation and aggregation, leukocyte-platelet interactions and other inflammatory processes. Subsequent smooth muscle cell (SMCs) migration and proliferation is followed by the formation and synthesis of extracellular matrix, giving rise to neointimal hyperplasia (NIH) [16]. Neointimal tissue is the result of SMCs migration and proliferation at the site of injury [135,136].

A healthy endothelium is crucial to maintain normal vascular tone. In physiological conditions, endothelium controls the exchange of macromolecules and oxygen between the blood and the underlying tissue [104]. In addition, it serves to regulate arterial reactivity through the synthesis and release of vasoactive mediators [137]. ECs also control the release of vasoconstrictors and vasodilators by sensing fluid shear stresses. In the case of endothelial destruction or dysfunction, the abnormal release of these vasodilators and vasoconstrictors changes the vascular tone and may promote the formation of a plaque [129,138].

Restoration of functional endothelial lining restores physiological vasomotion and inhibits further neointimal proliferation. However, despite several studies, the process and mechanism of endothelial regeneration remains poorly understood. In the 1970s, a number of studies reported the role of EC migration and proliferation from nearby un-injured ECs in the regeneration of endothelium at the site of injury [139,140]. However, other studies provided evidence to support the development of mature endothelial cells from the homing of endothelial progenitor cells (EPC) within the blood [141,142]. In the past decades, intensive effort has been undertaken to understand the biological properties of EPCs and their relevant contribution towards endothelial repair, but the results are still conflicting [137,143]. Some recent reviews suggest that EPC do not contribute directly to regrowth of the endothelium during the vascular healing process [137]. Perhaps, the only valid mechanism involved in EC regeneration is the proliferation and migration of the ECs from the edges of the injured area [137,144].

Both the degree of restenosis and the distribution of neointima along the length of the stent may be influenced by not only the endothelial growth rate [91] but also the origin of endothelial regeneration. In the current study, we report the variation of neointimal growth along the length of a stented artery *in vivo* through analysis of the variability in growth patterns from porcine coronary histological sections. The response of the stented artery

is simulated to provide *in silico* data from a two-dimensional computational model where two different re-endothelialisation scenarios were incorporated which focus on the effect of the origin of endothelial regeneration (random EC seeding and EC growth from proximal and distal ends). Results from these two different scenarios were then compared with the averaged trends of the *in vivo* data to identify the most probable mechanism of re-endothelialisation during vascular healing.

4.1 Animal Experiments

For the purpose of the current study, the arteries treated with BiodivYsio bare metal stents (3.5 x 15 mm) are taken into account. These animal experiments were performed according to UK home office regulations. The experimental protocol has been described in detail elsewhere [82,83]. A total of eight coronary arteries data has been used where stents were deployed in the right coronary arteries (RCA). Balloon pressure was kept at 8 atmospheric pressure for 30 seconds to allow the deployment of the stents. 2500 U heparin was injected before the interventional procedure and 150 mg of aspirin was administered orally for five days. Animals were sacrificed at 28 days post stenting and stented arteries were harvested from the animal. Arterial segments were cut into approximately 18-22 histological sections, as previously described [82,83]. Each section was investigated under a microscope and images of the histological section were saved digitally for post-processing (Figure 4.1A and 4.1B). The resolution of the microscope was kept constant for all sections and the scale at which images were saved was 3.22 μm/pixel.

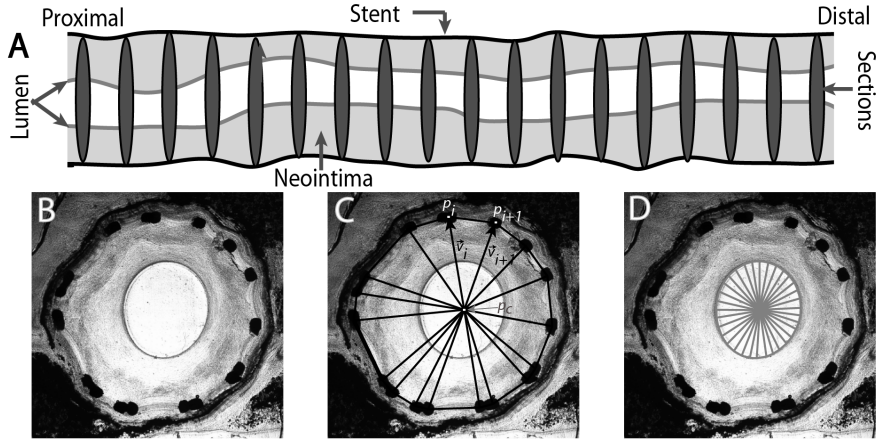

Figure 4.1: *Histological sections and post processing area calculations. (A) Idealised representation of the vessel where each circle represents one of the histology sections. (B) A representative histology section. Post-processing techniques to calculate (C) stent area and (D) lumen area.*

4.1.1 Post-Processing Method

The digital histology images were post-processed using MatLab (Mathworks, Inc.) to calculate stent, lumen and neointimal areas. The stent boundary was identified by manually selecting points at the centre of each stent strut, the lumen boundary was identified by manual identification of the lumen boundary. Both methods assume the area is bounded between points by a straight line. A centre point was identified and triangles were constructed for both stent (figure 4.1C) and lumen (figure 4.1D) by selecting two surface points and the centre point. The area of each triangle was calculated through the vector cross product method using the equation shown below:

$$Area = \frac{1}{2} |\vec{v}_i \times \vec{v}_{i+1}|$$

where $\vec{v}_i$ and $\vec{v}_{i+1}$ are the vectors pointing from the centre point P_c to point P_i and P_{i+1} respectively (Figure 4.1C).

$$Total\ area\ for\ a\ given\ section\ (stent\ or\ lumen) = \sum_{i=1}^{N} Area_i$$

where *N* denotes the number of triangles made from points in a given section. Neointimal area was obtained by subtracting lumen area from the stent area. As the measurement was a manual procedure it was repeated five times, for each section of every artery, to assess the errors involved in manual selection (Figure 4.2).

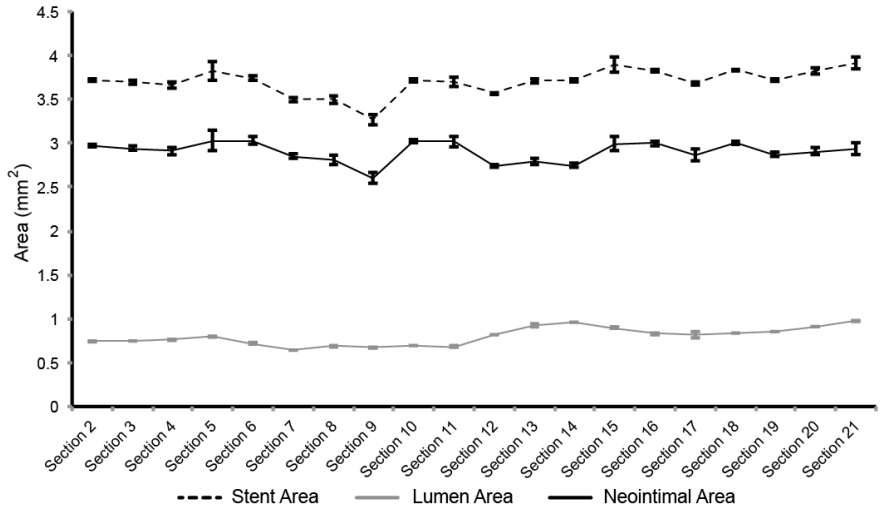

Figure 4.2: *Example of one artery showing a standard human error involved during the post-processing method for area calculations.*

4.2 Computational Model

A computational two dimensional multi-scale model of ISR has already been developed (chapter 1&2) [39,47,59] and has been

recently used to study the effect of re-endothelialisation rate and subsequent release of nitric oxide (NO) on the regulation of SMCs (chapter 3) [91]. In the current study, the vessel length has been increased by a factor of three compared to our previous model domains. Simulation of a longer vessel allows more stent struts to be deployed compared to our previous benchmark geometries allowing investigation of the morphological changes in neointima along the length of the stent under different endothelial regrowth scenarios. We considered a vessel of a length of 4.5 mm with a lumen width of 1 mm. The vessel wall thickness was defined as 120 μm, based on the average medial wall thickness observed in the histology sections. Six bare metal stent struts were deployed at a depth of 110 μm into the tissue, three into each side of the vessel wall.

In silico results were produced under two distinct re-endothelialisation scenarios. These scenarios represent possible behaviour of endothelial cell function following stenting as reported in the literature. The first scenario involves the regeneration of endothelial cells from either side of the stented region (the proximal and distal boundaries of the model) assuming complete endothelial denudation due to balloon angioplasty and stent deployment. This scenario of EC proliferation from both sides inward was highlighted by Itoh et al. [144], where the endothelium was completely denuded within the injured area. However, this complete removal of the endothelial layer was largely dependent on the experimental setup and the nature of endothelial damage. The second scenario, described previously in chapter 3 [91], involves random seeding of ECs, assumed to be a result of either endothelial patches remaining after the balloon angioplasty/stenting procedure and/or from homing of circulating endothelial progenitor cells to the site of injury. Harnek et al. [29] suggest there may be a small percentage of endothelium which remains following balloon assisted stent deployment but the exact location of these leftover patches is not known and the percentage of remaining endothelium appears to be stent design dependent [29].

For both scenarios it is assumed that 100% endothelium recovery occurs at 23 days post stenting, as previously described [91]. The obvious difference in the above scenarios is the evolution of the spatial distribution of endothelium on the inner layer of the vessel as a function of simulation time. Once the endothelium is present it is assumed to be able to sense the shear stress generated by the blood flow and produces NO based on shear stress magnitude. The concentration of NO is then used to inform the process of cell cycle arrest in the adjacent SMCs to maintain them in the quiescent state. If there is no endothelium present

adjacent to an SMC it will continue to proliferate, giving rise to neointimal development. In the current model no distinction is made between functional and non-functional endothelium, once endothelium has been generated it is assumed to immediately respond to shear stress stimuli. Therefore we assume that any endothelium which is not yet mature/functional does not play a significant role.

4.3 Results

4.3.1 In-vivo Results

The stent, lumen and neointimal areas were measured five times for each section of all arteries to obtain a measure of the error associated with post-processing, this error is shown for one artery in figure 4.2. The most proximal and distal sections were excluded from analysis as these sections were obtained very close to the end of the stent geometry and in some cases, an incomplete ring of struts excludes the possibility of computing the stent area. The number of sections in each artery were normalised to a fractional length of 1 along the stent as the x axis in the plot shown in figure 4.3A, with 0 corresponding to the first section analysed at the proximal end and 1 corresponding to the last section analysed on the distal side. The percentage stenosis due to neointima in each section was obtained using the mean value of stent area of each section from the five repeated measurements. The variation in percentage stenosis along the stent is shown for all eight RCA arteries in figure 4.3A. Comparison of the growth at the proximal and distal edges of all arteries indicates that six arteries showed higher neointimal growth at the distal end, with only two arteries showing equal or slightly lower neointima at the distal end. However, the difference in percentage stenosis between each end is not statistically significant ($p=0.16$). To better understand the growth trends, linear regression was applied to the neointimal area data for each artery to characterise the variation in slope from the proximal to distal ends. Analysis of the regression showed that almost all arteries have a small but positive slope except one where the slope was -0.00118 ± 0.0047 (neointimal area per normalised length whereas $\pm$ represents the standard slope error). However, it is also worthwhile to mention that some of the responses in figure 4.3A do not follow a straight-line trend and so linear regression may not be appropriate for all plots. The averaged value of the slope among all the arteries data was 0.035 ± 0.004 (neointimal area per normalised length). The averaged result from figure 4.3A is also shown in figure 4.3B where a slightly higher amount of neointimal growth on the distal side can be seen in comparison to the proximal side. Due to the size of deviation in the averaged neointimal response, it is rather difficult

to interpret the result though the overall growth response seems to stay fairly flat along the stent (figure 4.3B).

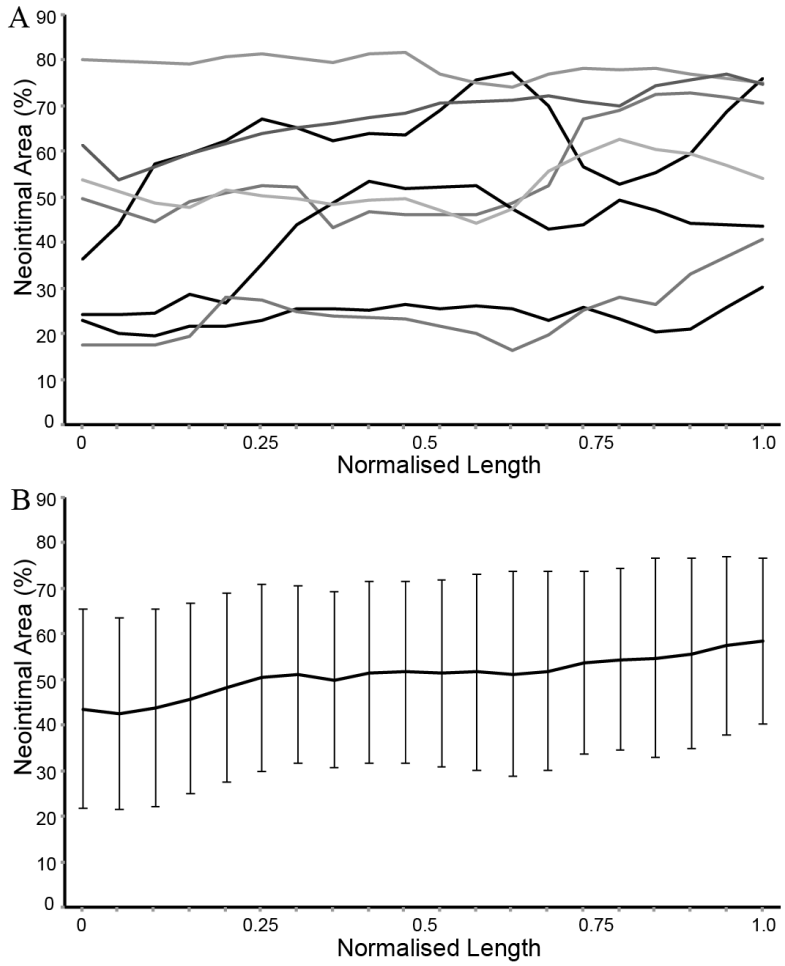

Figure 4.3: *In vivo variation in the percentage stenosis due to neointimal growth along the length of the stented segment, measured from histology. (A) Percentage of neointimal area in all eight RCA arteries (B) Averaged result of neointimal area percentage from all arteries shown in (A).*

4.3.2 Computational Model Results

Morphological differences in the simulated tissue growth patterns were observed between the two EC regeneration scenarios. The *in silico* results demonstrate a strong effect of the two extreme scenarios of EC regrowth. Random seeding of ECs resulted in a relatively homogenous distribution of neointima along the stented length (figure 4.4A) whereas the specification of endothelial growth from both sides results in a thicker neointimal lesion in the middle of the stented vessel (Figure 4.4B). These morphological

differences are clearly evident with the use of the same re-endothelialisation growth rate.

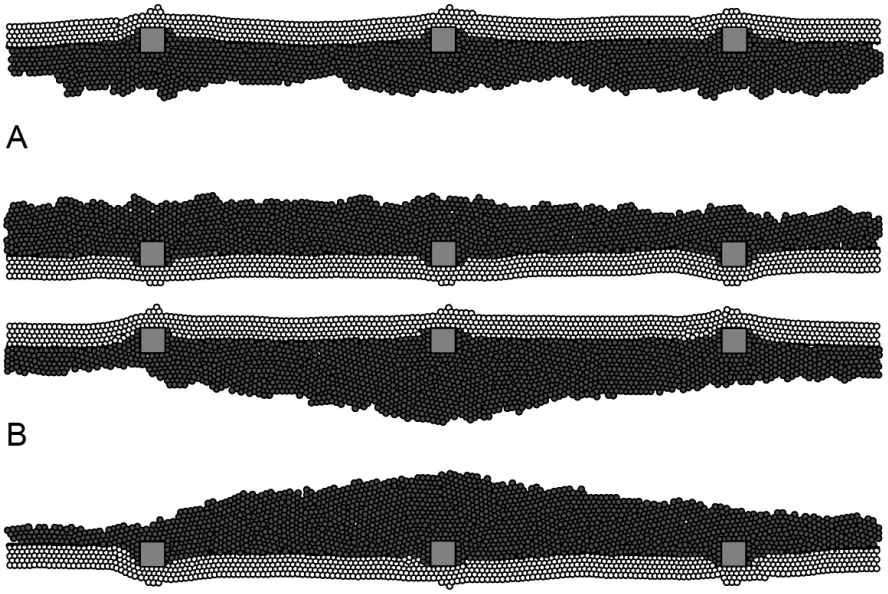

Figure 4.4: *Computational results showing qualitative morphological differences in neointimal growth between the two re-endothelialisation scenarios; (A) Random seeding of ECs and (B) inward EC growth from both sides. The six grey squares in each figure represent stent struts deployed in to the vessel. The tissue composed of white SMC cells underneath the struts shows the original vessel after stent deployment. However, dark grey SMCs represent the neointima in both scenarios.*

To compare with the processing applied to the *in vivo* data, the surface area of the stent, lumen and neointima are computed *in silico*. For the area estimation, rectangles were made with a height corresponding to the distance between the inner boundaries for both stent and lumen whereas the width of the rectangles is chosen to be equivalent to the diameter of one SMC (30 μm). For the height of the stent rectangle, centre points in the middle of struts are chosen (Figure 4.5A) similar to the measurements done in the *in vivo* data, however, for lumen, the inner most cells in the upper and lower half were identified within the width of the rectangular window and distance between those two point was calculated (Figure 4.5A). The area of the rectangles is computed by multiplying width with the height. These rectangles, both stent and lumen with a width equivalent to one SMC diameter, were moved from proximal to the distal end using a step size of 30 μm in order to compute the area along the axial direction. Stent, lumen and neointimal area computed *in silico* are shown in Figure 4.5B and 4.5C where neointimal area is obtained by subtracting the lumen area from the stent area. The neointimal

area trends (from proximal to the distal end) are significantly different, especially in the centre of the stented area and at the extremes (proximal and distal ends). As for the *in vivo* results, the percentage stenosis was calculated and is shown in Figure 4.6 along with the standard deviation of results obtained from six simulation runs. Figure 4.6 clearly shows a distinct peak in the middle of the stented vessel when EC regeneration is assumed to occur from both sides, with the random seeding scenario resulting in a more homogeneous (less pronounced peaks) neointimal growth within the vessel*.*

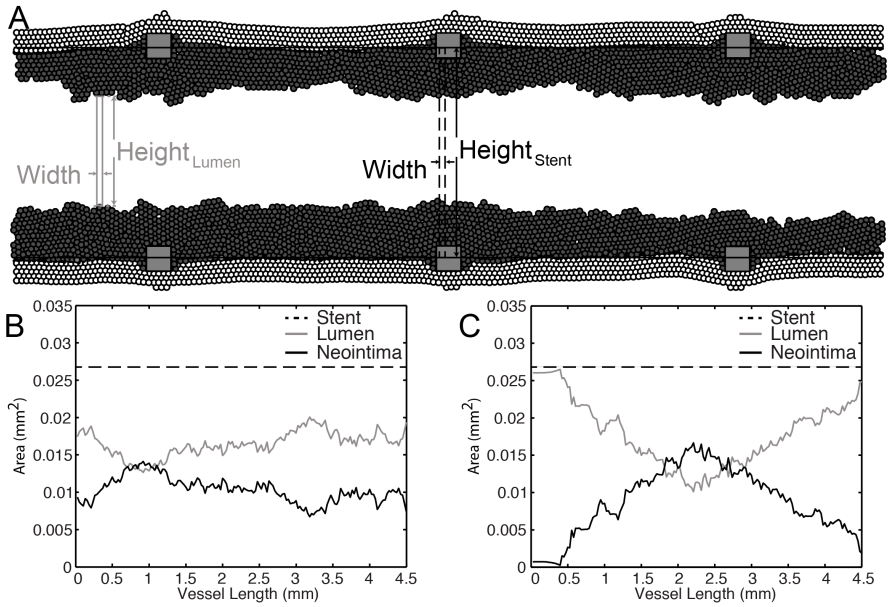

Figure 4.5: *Area of the stent, lumen and neointima along the length of the stented region computed in silico. (A) surface area measurement procedure to calculate stent and lumen areas by making rectangles using the stent and lumen boundaries. Neointimal area is obtained by subtracting lumen area from the stent area, (B) Random seeding of ECs and (C) ECs re-growth from both sides inwards.*

4.3.3 Histological and simulation results comparison

To compare the two *in silico* endothelial regeneration scenarios with the *in vivo* results to examine how well each scenario agrees with the growth trends observed from histology, the ratio of neointimal area at each location relative to that at the centre of the stented section was calculated. These ratios are defined as:

$$Ratio_{proximal\ to\ centre} = \frac{Neointimal\ Area\ N}{Neointimal\ Area\ at\ proximal\ end}$$

$$Ratio_{distal\ to\ centre} = \frac{Neointimal\ Area\ N}{Neointimal\ Area\ at\ distal\ end}$$

Where neointimal area *N* is the neointimal area at each histological section. So a uniform growth will give a straight line at 1 and any deviation from ratio=1 will suggest more or less growth at either end.

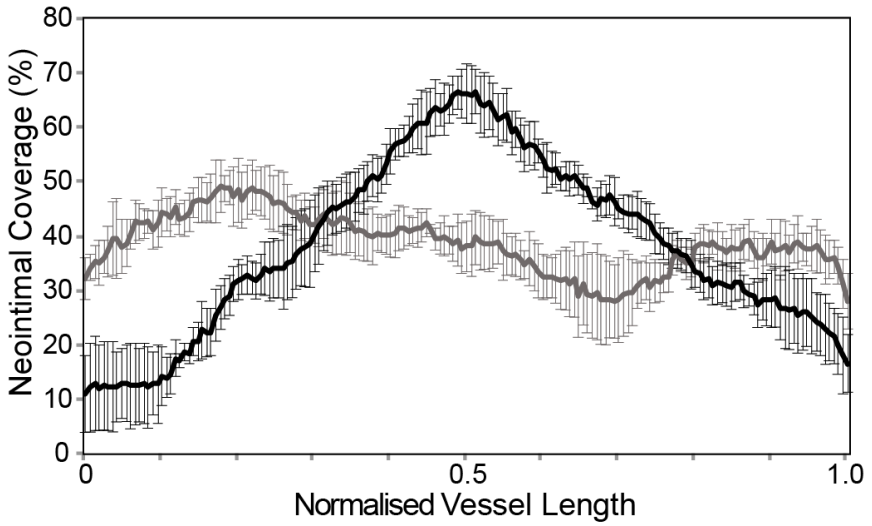

Figure 4.6: *Percentage of neointimal growth based on the stent area after deployment for both re-endothelialisation scenarios. Grey solid line shows the scenario of random EC seeding whereas black solid line represents neointimal growth based on EC growth from both sides.*

Figure 4.7A and 4.7B display the averaged outcome of proximal to centre and distal to centre ratio calculations respectively for all the arteries along with the modelling results of both endothelium scenarios. It is clear from figure 4.7 that the variation in the animal RCA arteries remains fairly smooth. In comparison to the histological data, the assumption of random EC regrowth shows close qualitative resemblance with the animal data and the growth along the stented length in that setting tends to remain moderately flat. However, figure 4.7 also strongly suggests that the neointimal ratio from the animal data does not support the hypothesis of the inward endothelium regrowth that results in reasonably higher centre to side ratios and dictates a higher neointima in the middle of the stented vessel. For ratio calculations, different reference points (ratio from centre to sides, or from sides to centre etc.) can be used but the overall conclusion, showing a disagreement of the EC from both side scenario with the random EC and *in-vivo* data, remains true. The ratio plots of EC growth from both sides initially follow the *in vivo*

data and random EC growth scenario trends near the reference point, but then it starts to deviate marginally (Figure 4.7).

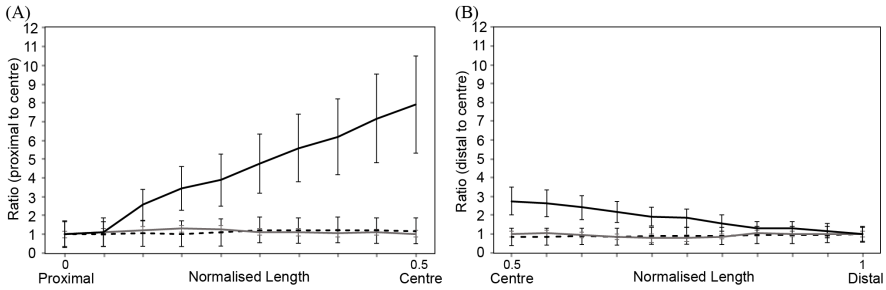

Figure 4.7: *Comparison of the ratio trends between the animal data and two endothelium re-growth modelling scenarios based on the percentage of neointima inside the vessel. (A) ratio from proximal to the centre and (B) ratio from distal to the centre. Black dotted line represents the in vivo data, solid grey line represents in silico random EC scenario and black solid line represents in silico EC from both sides scenario.*

4.4 Discussions

Porcine experiments have been helpful to understand the dynamics of the complex restenotic process and the underlying mechanisms. Combining such data with the outcomes from numerical simulations can inform understanding of such processes and allows the testing of new hypotheses. Evaluation of the dynamics of endothelial growth or repair processes and the subsequent influence of this on ISR development still seems to be lacking in the literature. To our knowledge, there has been only one *in vivo* study undertaken by Itoh et al [144] in the pial arteries of mice to specifically investigate the re-endothelialisation process. In that study, a region of the endothelium was damaged via the photochemical reaction of rose bengal to green laser light. Tie2-green fluorescent protein was used as a marker to identify live ECs. It was observed that the endothelium recovery process had already started within the first 24 hours following endothelial injury and regeneration of the endothelium was observed from both edges (proximal and distal) of the denuded artery. Moreover, faster endothelial growth was observed from the proximal edge in comparison to the distal end and the meeting point of endothelial layers from both sides was always distal to the centre of the injury, suggesting the differences in the re-endothelialisation rate. The difference in the growth rate was due to flow direction where ECs were observed more elongated towards the flow direction and migrated and proliferated faster. Any apparent involvement of foreign progenitor cells in the EC repair process was not found, however this could be related to the experimental setup that was used in the study. Additionally, It is also worthwhile to mention that though the findings of Itoh et al. [144] are essential to

understand the endothelium regrowth process, their model and setup is not clinically relevant to the vascular stent induced injury models and results may not be extrapolated directly to the coronary stenting experiments. The clinically irrelevant model highlights the need to perform similar experiments in the porcine coronary stented arteries in order to evaluate the endothelium regrowth process.

We have used the findings of Itoh et al [144] to describe one possible re-endothelialisation scenario, assuming that ECs become functional in a similar fashion as they re-generate to form a lining on the vessel wall. Our modelling approach predicts that, under this scenario, neointimal growth in such an artery will result in a greater stenosis at the location where these edges meet each other. If both the findings shown by Itoh et al. [144] and the interactions between endothelial cells, flow and smooth muscle cells assumed in the model are representative of *in vivo* conditions, then the histological data shown in Figure 4.2, 4.3 and 4.7 are expected to show a peak in the growth process either at the centre of the stented vessel (based on our computational model assumption of identical growth rates at both proximal and distal sides) or somewhere distal to the centre (based on the observation of Itoh et al. [144]). However, the histological data does not seem to support the notion of EC inward growth alone as suggested by Itoh et al [144]. The *in vivo* data presented here shows stronger support for the scenario where endothelial regeneration occurs inside the stented region. In the biological experiments reported here endothelial regeneration may include the involvement of both methods of EC regeneration (EC growth from both sides and from random patches / progenitors) acting together, as a result further controlled biological experiments are required to confirm the detail of this process.

This opens up another question. Do progenitors appear inside the vessel? Several studies have reported that endothelial regeneration is not mediated by the homing and differentiation of EPCs into mature ECs [137,144,145,146,147], however, they may facilitate the migration, elongation and proliferation of the resident ECs [144]. But, as we have shown, taking these observations into account and considering only that endothelium grows from both sides of the injury, we end up in a peak-scenario that does not coincide with the neointimal growth patterns observed in the histology. According to Harnek et al, a little endothelium in the denuded artery may survive the trauma caused by the balloon assisted stent deployment, so these patches may also contribute towards re-endothelialisation. The *in vivo* study done by Itoh et al. [144] does not include the presence of healthy patches; instead they induce a complete endothelial

injury in the selected area of the vessel and the same approximation was taken in our computational model and this may explain the difference in results.

Another important observation from the evaluation of the histological neointimal growth reveals that a slightly higher growth was observed on the distal end when compared with the proximal side. This has been shown by linear regression analysis and a positive slope was observed in all the cases. Although, a mismatch in stent-vessel size at distal end resulting in deeper injury may account for exaggerated neointimal proliferation, it may also be due to the effect of the direction of flow on the endothelium regrowth process that mediates a faster growth from the proximal side of the injury and may also involve the flow direction dependent growth from the leftover healthy patches. ECs directional migration and faster growth in the direction of flow has already been observed in several studies where EC become more elongated and proliferated faster in the flow direction however, these studies do not focus on the neointimal growth [144,148,149].

The current computational study is limited only to 2D ISR model and there is no direct comparison possible in terms of vessel dimensions (length and diameter) *in vivo* and *in silico* along with the differences in the number of struts present within the stented length, however the aspect ratio (length vs diameter) of the vessel was kept quite similar in the *in silico* model (4.5:1) to that seen in the *in vivo* experiments (4.55:1). A better comparison should be done with the ISR3D model using more realistic 3D idealised vessels. The final goal of such studies to better understand the ISR patterns will be to include the vascular geometry that can be obtained directly from the imaging modalities and should be incorporated in the ISR3D model. This will allow us to model the blood flow in a more realistic domain taking into account the curvature of the vessel along with the accurate stent design. Modelling ISR in such realistic domains may better correlate with the neointimal patterns seen in the histology and allow us to do quantitative comparison which is far from trivial until now and should be taken as a next step forward in this research.

Finally, our study suggesting endothelial regeneration potentially from patches of surviving EC cells has potential clinical relevance. Stents vary in their design (open cell vs. closed cell), strut dimensions (thickness and width), and metal to artery wall ratio. All these factors can influence the size of surviving EC patch and hence endothelial regrowth. It can partially explain the difference in endothelial coverage among 1st generation and newer stents

and may also help clinicians in making a more informed choice on selecting a particular stent for a patient and to develop better stents in future. Further studies with different stents are warranted.

4.5 Conclusions

Using computational model of ISR and comparison with *in vivo* histology we conclude that, within the context of the assumptions involved in the modelling process, endothelial growth from regions of the vessel proximal and distal to the stent is not sufficient to explain the morphology observed from histology. The results suggest that random EC seeding and/or patches of endothelium that survive balloon expansion and stent deployment play a role in endothelial recovery.